

Chapter 7

The ISOGAL survey and the completeness analysis

7.1 Introduction

The ISOGAL project is an ISO infrared survey of specific regions in the Galactic Plane, which were selected to provide information on Galactic structure, the stellar populations and mass-loss, and the recent star formation history of the inner disk and Bulge of the Galaxy. Several (about 25) scientific papers have been published based on the ISOGAL data. They present studies of the Galactic structure, an analysis of the complete AGB population, and studies of infrared dark clouds and young stellar objects (Omont et al. 2003).

The survey was performed at 7 and 15 μm with ISOCAM, covering 16 square degrees with a spatial resolution of 3-6'' and a sensitivity of 10-20 mJy, two orders of magnitude deeper than IRAS at 12 μm , and a factor 10 deeper than the MSX A band (8 μm).

The 7 and 15 μm ISOGAL data were combined with the I , J , K_s (effective wavelengths 0.79, 1.22 and 2.14 μm) ground-based data from the DENIS survey, resulting in a 5-wavelength catalogue of point sources. The combination of mid- and near-infrared measurements permits a determination of the nature of the individual sources and of the interstellar extinction towards them.

A complete overview of the first scientific results from ISOGAL data is given by Omont et al. (2003), while the description of the point source catalogue is given in an Explanatory Supplement (Schuller et al. 2003).

In the present chapter I will briefly describe the survey and then I will move to the description of the ISOGAL completeness analysis (Sect. 1.4 below), to which I contributed significantly.

7.2 Observations

The ISOGAL observational program –250 hours of observing time– is one of the largest ISO programs. The ISOCAM observations were taken from January 1996 to April 1998, i.e., over the whole ISO mission.

The observed fields ($\sim 16 \text{ deg}^2$) are distributed along the inner Galactic Disk, mostly within $|\ell| < 30^\circ$, $|b| < 1^\circ$, as shown in Figure 1.

Chapter 7: The ISOGAL survey and the completeness analysis

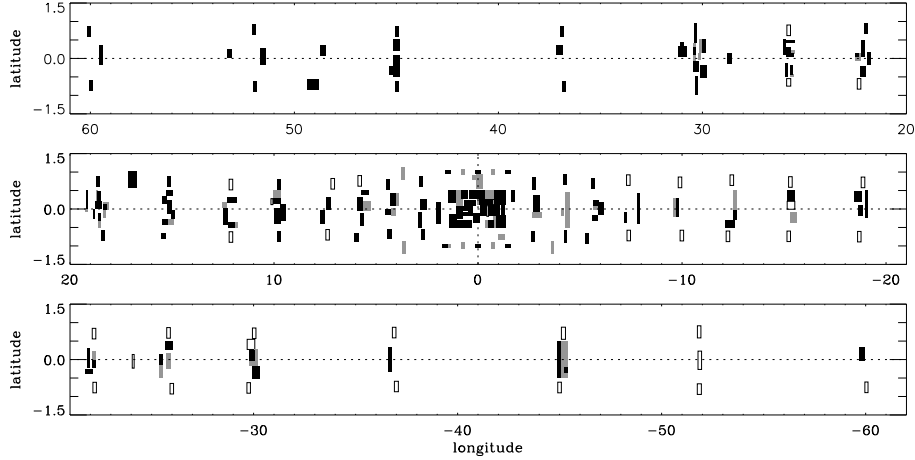


Figure 7.1: Galactic map of ISOGAL fields with $|\ell| < 60^\circ$. Black, grey and open boxes show fields which have been observed at both 7 & 15 μm , at 7 μm only and at 15 μm only, respectively. Twenty-one additional northern fields (not displayed) were also observed, at $\ell \approx +68^\circ, +75^\circ, +90^\circ, +98^\circ, +105^\circ, +110^\circ, +134^\circ, +136^\circ, \& +138^\circ$. Figure adapted from Schuller et al. (2003).

Detailed information on the observation parameters and on the field positions is available in the ISOGAL Explanatory Supplement (Schuller et al. 2003) and on the ISOGAL web server www-isogal.iap.fr/.

Most of the observations were performed with the broad filters *LW2* and *LW3* and a pixel scale of $6''$. A few regions around the Galactic centre were observed with the narrow filters *LW5* or *LW6*, and *LW9* and a pixel scale of $3''$, to reduce the effects of bright sources that would saturate the detector (thus moving the saturation limit from $Flux_{12} > 6 \text{ Jy}$ to $Flux_{12} > 20 \text{ Jy}$). A list of the ISOCAM filters used for the ISOGAL survey is given in Table 7.1.

The observations, performed in raster mode ($\sim 0.1 \text{ deg}^2$), were oriented in Galactic coordinates. At each raster position 19 basic ISOCAM frames (32×32 pixels) were taken, resulting in a total integration time of 21 s per raster position. The raster steps were typically $90''$ in one direction and $150''$ in the other direction, and each sky point was observed for a maximum of 4 times, with an average of 1.5. Only 384 of the 463 raster positions were used for the production of the first ISOGAL point source catalogue, because only one raster was used in case of overlapping areas to avoid redundancy. The total number of ISOGAL fields (rectangular area of the sky whose edges are aligned with the galactic axes and observed by ISOGAL) is 263. They can be divided in 43 fields (FA) only observed at 7 μm , 57 fields (FB) only observed at 15 μm , and 163 fields (FC) observed at both 7 and 15 μm .

Systematic cross-identification with the near-infrared *I, J, K_s* sources of the

Table 7.1: ISOCAM filters used for ISOGAL: reference wavelengths and bandwidths, zero point magnitudes and flux densities, and total observed area. Table adapted from Schuller et al. (2003).

Filter	λ_{ref} [μm]	$\Delta\lambda$ [μm]	ZP ^a [mag]	$F_{mag=0}$ [Jy]	Area [deg ²]
LW2	6.7	3.5	12.39	90.36	9.17
LW5	6.8	0.5	12.28	81.66	0.64
LW6	7.7	1.5	12.02	64.27	2.97
LW3	14.3	6.0	10.74	19.77	9.92
LW9	14.9	2.0	10.62	17.70	3.53

^aThe magnitude of a source with a flux density F_ν , expressed in mJy is given by $mag = ZP - 2.5 \times \log(F_\nu)$

DENIS survey was an integral part of the ISOGAL program and special DENIS observations were performed for this purpose (Simon 2004). DENIS data were available for 95% of the fields surveyed with ISOCAM.

7.3 Data processing and analysis

Data reduction was performed with standard procedures of the CAM Interactive Analysis Package (CIA version 3). A sophisticated pipeline was developed for the ISOGAL data (Schuller et al. 2003), which involves more steps than the standard treatment of ISOCAM data (see ISOCAM Handbook, Blommaert et al. 2003). This was necessary because of the extreme conditions of the ISOGAL observations. In addition to the usual problems, i.e. glitches, dead pixels and the time-dependent behaviour of the detectors, one needs also to consider bright background emission, crowding, high spatial density of bright sources (which causes pixel-memory effects), and the short integration time.

The point sources were extracted using a dedicated PSF fitting routine (Schuller et al. 2003).

The completeness of point source extraction has been systematically addressed through retrieval of artificial sources, which is described in the next section.

7.4 Artificial sources

Synthetically reproducing the complete process of photometric measurements is the only way to properly characterise all undesired effects associated with observations in a crowded field.

An artificial star experiment consists of adding artificial stars to ISOGAL images, and re-extracting all point sources with the same pipeline as the one used to generate the ISOGAL catalogue. The analysis of input magnitudes of artificial

sources with those in output enables one to characterise the effects of crowding on the photometric quality and the completeness of the extracted point source catalogue.

Artificial star experiments were conducted on ISOGAL images following a procedure similar to that applied by Bellazzini et al. (2002):

- The magnitude of artificial stars was randomly extracted from the observed luminosity function.
- The goal of the procedure is to study the effects of crowding. Therefore, it is of primary importance that the artificial stars do not interfere with each other. The interference between artificial stars would, in fact, change the actual crowding and affect the results of the artificial experiment study. To avoid this serious bias, one can divide the image (or raster in the ISOGAL case) into grids of cells of known width (20 pixels). One artificial star is randomly positioned in each cell, avoiding the border of the cell in order to control the minimum distance between adjacent artificial stars.
- The stars were simulated using the point-spread-function (PSF) determined directly from the average ISOGAL data corresponding to the observational setup (filter, pixel scale). A new image was then built by adding the artificial stars and their Poisson photon noise into the original raster image.
- The measurements process was performed in the same way as the original measures.
- The output magnitudes were recorded, as well as the positions of the lost stars.
- To generate a significant number of artificial stars, for each image, the whole process was repeated between 100 and ~ 300 times, depending on the source density and image size. A total of 5×10^3 to 4×10^4 sources were generated.

As an example, figure 7.2 shows the differences between input and output magnitudes, $mag_{input} - mag_{output}$, obtained for the raster TDT=83600913 (filter=LW2, pixel scale $6''$), which is centred at longitudes 1.37° and latitude -2.63° , covers a region of $0.22 \times 0.24^\circ$, and has a density of 6660 sources per deg^{-2} . A number of 55 artificial star were added each run and a total of 350 runs were performed.

The distribution of the difference is not symmetric. There is a strong concentration at zero, but also a positive tail of stars. This means that the output magnitudes are brighter than the input ones and this is due to the blending between artificial stars and real stars. When an artificial star is blended with a fainter source its output magnitude will be brighter than its input magnitude because of the flux contributed by the fainter blended source. Artificial sources having an output magnitude +0.75 mag brighter than their input magnitude were considered lost. In fact, if at the position of the artificial star one measures a point source more than 0.75 mag brighter than the magnitude of the input artificial star, this

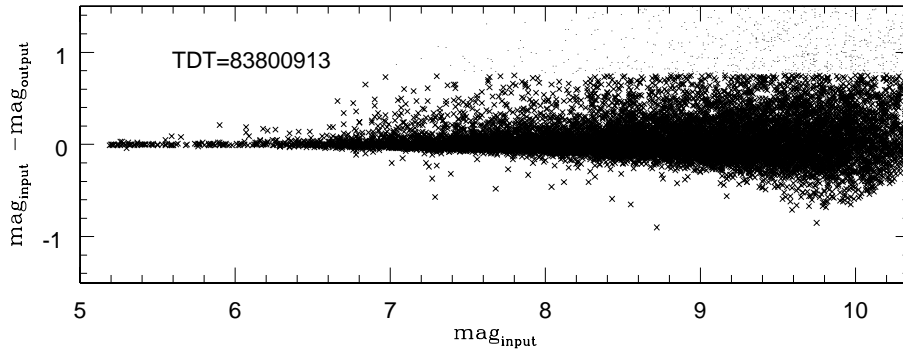


Figure 7.2: Differences between the input and output magnitudes of the 19250 artificial stars vs. input magnitudes for the raster TDT=83600913. If the difference is larger than 0.75 mag the artificial star is considered lost.

means that the artificial star falls on a brighter real source and in this case the star actually recovered is the real one.

Artificial star simulations were conducted on 35 images (total area $\sim 2 \text{ deg}^2$) selected to have all possible observational setups and different crowding levels (the source density ranges from 0.0017 to 0.03 sources per pixel). Artificial star experiments were used to evaluate both random and systematic photometric errors due to crowding, as well as the completeness level of the extraction as a function of source density.

Output magnitudes were generally found to be brighter than input magnitudes. This bias is very small for bright stars, but can reach 0.3 magnitude for the faintest ones in the densest fields, where the probability of blending with real stars is higher (see Fig. 7.3).

The completeness of the extraction was quantified by analysing for each simulation the fraction of retrieved simulated sources as a function of input magnitude. A smooth curve appears which drops at faint magnitudes. The magnitude where this fraction becomes less than 50% depends on the density of the field. The point source catalogues extracted from the various ISOGAL rasters were found at least 50% complete down to the faintest end in fields with low stellar density, but this was not the case in denser regions.

For each observational setup (combination of pixel scale and filter) a relation between the estimated 50% completeness limit and the field source density was derived and used to define the limiting magnitude of each ISOGAL observation, corresponding to the faintest sources that were included in the published catalogue. The completeness limit depends on the source density, on the intensity and the structure of the local diffuse background, and on the filter. The sensitivities reached at 7 and 15 μm for standard ISOGAL conditions are summarised in Table 7.2.

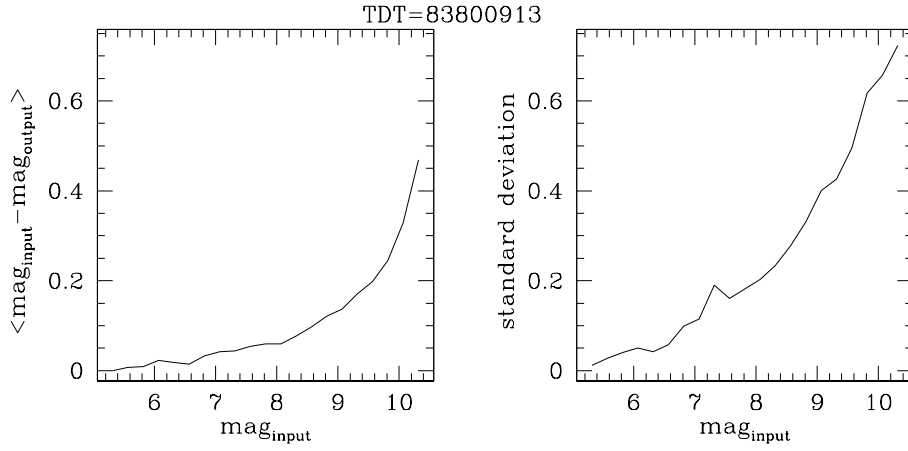


Figure 7.3: **Left-panel:** Mean differences between the input and recovered magnitudes per bin of input magnitude, relative to the 19250 artificial stars simulated for the raster TDT=83600913. **Right-panel:** Standard deviation of the differences between the input and recovered magnitudes as a function of the input magnitude.

Table 7.2: Sensitivities¹ at 7 and 15 μm for typical ISOGAL conditions . Table adapted from Omont et al. (2003).

Region ²	Source density	Background	Pixel	Filter	7 μm		15 μm	
					mag	flux (mJy)	mag	flux (mJy)
A	low	weak	6''	broad	10	9	8.7	7
B	high	moderate	6''	broad	9	22	8	12
C	very high	strong	3''	narrow	8.4	35	7	30
D	high	very strong	6''	narrow	7.7	55	6.5	45

¹ Sensitivity limits of ISOGAL sources published in PSC *Version 1*, corresponding approximately to detection completeness of 50% (Schuller et al. 2003).

² Typical regions:

A Lowest density Bulge fields, $|b| \geq 2^\circ$

B Standard Disk fields, $|b| < 0.5^\circ$, $|\ell| \leq 30^\circ$

C Central Bulge/Disk fields, $|b| < 0.3^\circ$, $|\ell| \leq 1^\circ$

D Most active star formation regions such as M16, W51.

7.5 Concluding remarks

The distribution of limiting magnitudes, for all ISOGAL observations is shown in Fig. 7.4. Since most observations were done with the broad *LW2* and *LW3* filters, these histograms show that the typical reached sensitivity is around 20 mJy at 7 μm and 12 mJy at 15 μm .

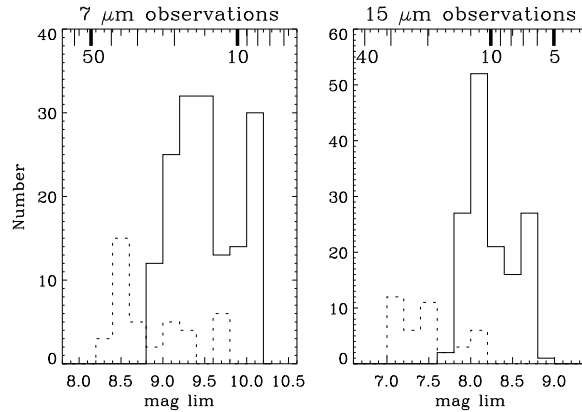


Figure 7.4: Distribution of the magnitudes at which the catalogues become incomplete at the 50% level for the broad filters *LW2* and *LW3* (full lines), and for the narrow filters (dotted lines). The logarithmic scales at the top of each panel show the corresponding flux densities in mJy for *LW2* and *LW3*. A small correction has to be applied for the corresponding flux densities with narrow filters. Figure adapted from Schuller et al. (2003).

About $\approx 25\%$ of extracted point sources fall below these magnitude limits. Analysing the quality flags of discarded sources, the photometric cut is far more severe for moderate quality sources than for good quality ones.

The completeness findings have been complemented and checked by the results of several repeated observations (in one case with $3''$ pixels, rather than the typical $6''$ pixels, and hence with greatly reduced crowding), and by comparison with DENIS (or 7 μm) red giant source counts.

7.5 Concluding remarks

In summary the ISOGAL PSC (version 1.0) contains 106 150 sources. It gives I, J, K_s , [7], [15] magnitudes, at five wavelengths (0.8, 1.25, 2.15, 7 & 15 μm); DENIS associations (I,J, K_s) are given when available. About half of the sources have 7-15 μm associations and 78% have DENIS associations. Quality flags are provided for each source at each wavelength, as well as for source associations, and only sources with a reasonable quality and with a magnitude above the 50% completeness limit are included in the catalogue (Schuller et al. 2003).

Chapter 7: The ISOGAL survey and the completeness analysis

Acknowledgements. I am grateful to all members of the ISOGAL consortium, in particular to Prof. Alain Omont from the Institute d'Astrophysique de Paris, P.I. of the survey, and to Frederic Schuller for their collaboration. "Grazie molto" to Paolo Montegriffo for the fruitful discussions on the completeness analysis.

References

- Bellazzini, M., Fusi Pecci, F., Montegriffo, P., et al. 2002, *AJ*, 123, 2541
Blommaert, J. A. D. L., Siebenmorgen, R., Coulais, A., et al., eds. 2003, *The ISO Handbook, Volume II - CAM - The ISO Camera*
Omont, A., Gilmore, G. F., Alard, C., et al. 2003, *A&A*, 403, 975
Schuller, F., Ganesh, S., Messineo, M., et al. 2003, *A&A*, 403, 955
Simon, G. 2004, in preparation